Title

NLRP3 inflammasome activation results in hepatocyte pyroptosis, liver inflammation, and fibrosis in mice.

Journal

Hepatology (Baltimore, Md.), 59(3)

ISSN

0270-9139

Authors

Wree, Alexander
Eguchi, Akiko
McGeough, Matthew D
et al.

Publication Date

2014-03-01

DOI

10.1002/hep.26592

Peer reviewed

Published in final edited form as:
Hepatology. 2014 March ; 59(3): 898–910. doi:10.1002/hep.26592.

NLRP3 inflammasome activation results in hepatocyte pyroptosis, liver inflammation and fibrosis

Alexander Wree[1,2], **Akiko Eguchi**[1], **Matthew D. McGeough**[1], **Carla A. Pena**[1], **Casey D. Johnson**[1], **Ali Canbay**[2], **Hal M. Hoffman**[1,3], and **Ariel E. Feldstein**[1,3]

[1] Department of Pediatrics, University of California – San Diego, 9500 Gilman Drive, La Jolla, USA

[2] University Hospital Essen, Department of Gastroenterology and Hepatology, Hufelandstrasse 55, 45122 Essen, Germany

[3] Rady Children's Hospital of San Diego

Abstract

Inflammasome activation has been recently recognized to play a central role in the development of drug-induced and obesity-associated liver disease. However, the sources and mechanisms of inflammasome mediated liver damage remain poorly understood. Our aim was to investigate the effect of NLRP3 inflammasome activation on the liver using novel mouse models. We generated global and myeloid cell specific conditional mutant Nlrp3 knock-in mice expressing the D301N Nlrp3 mutation (ortholog of D303N in human *NLRP3*) resulting in a constitutively activated NLRP3. To study the presence and significance of NLRP3 initiated pyroptotic cell death, we separated hepatocytes from non-parenchymal cells and developed a novel flow cytometry-based (FACS) strategy to detect and quantify pyroptosis *in vivo* based on detection of active caspase1 and propidium iodide (PI) positive cells. Liver inflammation was quantified histologically, by FACS and via gene expression analysis. Liver fibrosis was assessed by Sirius-Red-staining and qPCR for markers of hepatic stellate cell-(HSC)-activation. NLRP3 activation resulted in shortened survival, poor growth, and severe liver inflammation; characterized by neutrophilic infiltration and HSC-activation with collagen deposition in the liver. These changes were partially attenuated by treatment with anakinra, an interleukin-1 receptor antagonist. Notably, hepatocytes from global Nlrp3 mutant mice showed marked hepatocyte pyroptotic cell death with more than a fivefold increase in active caspase1-PI double positive cells. Myeloid cell restricted mutant NLRP3 activation resulted in a less severe liver phenotype in the absence of detectable pyroptotic hepatocyte cell death.

Conclusions—Our data demonstrates that global and to a lesser extent myeloid-specific NLRP3 inflammasome activation results in severe liver inflammation and fibrosis, while identifying hepatocyte pyroptotic cell death as a novel mechanism of NLRP3 mediated liver damage.

Address for correspondence Ariel E. Feldstein, M. D., Professor of Pediatrics Department of Pediatrics University of California San Diego 9500 Gilman Drive, MC 0715 La Jolla, CA. 92037-0715 USA Tel: + 1 858 966 8907 Fax: + 1 858 966 8917 afeldstein@ucsd.edu.

Conflict of Interest: Dr. Hoffman is a consultant for SOBI, Regeneron, and Novartis.

Keywords

NLRP3; inflammation; liver fibrosis; pyroptosis; hepatocyte

Introduction

Inflammasomes are multi-protein cytoplasmic complexes that serve as pattern recognition receptors.[1] They intersect with a wide variety of immune and cell death pathways. NLRP3, the most well studies Nod like receptor, forms a complexes comprised of adaptor proteins such as the apoptosis associated speck like protein (ASC), and the serine protease caspase-1(Casp1). NLRP3 inflammasome activation governs the cleavage and activation of Casp1 resulting in maturation of effector pro-inflammatory cytokines such as pro-IL-1β and pro-IL-18.[2-4]

Casp1 is activated from a 45 kDa inactive precursor that contains a 15kDa N-terminal subunit, a central 20 kDa subunit, a 10 kDa c-terminal subunit.[5-6] The active Casp1 is comprised of a tetramer consisting of two 20 kDa fragments and two 10 kDa fragments.[7] Once activated, Casp1 is then able to cleave a variety of protein precursors affecting the cytoskeleton of the cell, glycolysis, mitochondria function, and inflammation.[8-9] Other studies indicate that Casp1 may be important in promoting survival upon pathogen attack as well as having a more general role as a regulator of lipid metabolism.[10] Casp1 activation can also directly induce a distinct form of programmed cell death called pyroptosis.[11-12] Although, pyroptosis has been well described *in vitro*, its relevance *in vivo* has remained unclear and supported mainly by indirect reports demonstrating Casp1 mediated effects independent of IL-1β and IL-18 secretion. As in apoptotic cell death, cells undergoing pyroptosis incur DNA damage and become positive in the TUNEL assay. However, in contrast to apoptosis, pyroptosis is also associated with cell swelling, release of pro-inflammatory intracellular contents and pore formation in the cell membrane, thereby becoming positive for propidium iodide (PI) staining.[13-14]

We, and others, have recently shown that hepatic Casp1 activation occurs in both Bone Marrow-derived Kupffer Cells (macrophages) and hepatocytes during the development of nonalcoholic steatohepatitis (NASH) and alcoholic steatohepatitis (ASH) and this activation appears to be mediated through the NLRP3 inflammasome.[15-17] These studies demonstrate that Casp1 plays an important role in inflammation and fibrosis during NASH and ASH development.[15, 18] Furthermore, treatment with an interleukin-1 (IL-1) receptor antagonist has been shown to ameliorate ASH in mice.[10] However, the specific contribution of persistent NLRP3 inflammasome activation in hepatic parenchymal versus non-parenchymal cells to liver pathology *in vivo* and the molecular mechanisms involved in this process remain incompletely understood. To address these issues, we have generated two novel mouse models with global, or myeloid-specific, expression of a mutant constitutively activated NLRP3-inflammasome.[19-20]

Materials and Methods

Generation of NLRP3 knock-in mice

We generated, as previously described, an Nlrp3 knock-in mouse strain with an aspartate 301 to asparagine (D301N) substitution, which corresponds to the D303N mutation seen in human cryopyrin associated periodic syndromes (CAPS).[20] This point mutation is thought to cause a conformational change that confers ligand-independent constitutive activation of the mutated NLRP3 inflammasome. Briefly, the targeting construct pPNTlox2PNlrp3D301N was created by cloning 4–7 kb regions directly upstream and downstream of a targeted position in intron 2 of *Nlrp3* around the neoR antibiotic resistance cassette in plasmid pPNTlox2P (Fig. 1).[19] Due to the presence of an intronic floxed neomycin resistance cassette, the expression of the mutation does not occur unless the Nlrp3 knock-in mice (*Nlrp3*^{D301NneoR}) are first bred with mice expressing Cre recombinase. Floxed mice were bred to mice expressing Cre recombinase under control of zona pelucida 3 (CreZ: universal expression of D301 mutant Nlrp3)[21] or lysozyme (CreL: D301N expression in myeloid lineage cells only).[22]

Mouse strains

The *Nlrp3*^{D301NneoR} mice used in this study are now available from Jackson Labs as B6N.129-*Nlrp3*^{tm3Hhf}/J. Strains C57BL/6-Tg(Zp3-cre)93Knw/J and B6.129P2-*Lyz2*$^{tm1(cre)Ifo}$/J were both acquired from Jackson Labs. Mice were cared for in accordance with appropriate institutional guidelines. Experimental protocols were approved by the UCSD Institutional Animal Care and Use Committee.

Anakinra treatment

To assess the role of interleukin-1 receptor (IL-1R) signaling within the generated mouse models we treated Nlrp3 CreZ knock-in mice with an IL-1 receptor antagonist (anakinra). The drug or saline injections at a comparable volume were subcutaneously injected daily at a dose of 300 mg/kg from day 2 to day 13.

Liver sample preparation

Nlrp3 CreZ mice were sacrificed at day 12-14 after birth while the mother remained on a normal diet. Liver tissue was harvested under deep anesthesia and divided: (a) a representative section was fixed in 10% formalin for 24h and embedded in paraffin, (b) another representative section was snap frozen in isopentane, submerged in liquid nitrogen and embedded in O.C.T. (c) samples of 50μg were placed in 0.5ml of RNAlater® Solution (Lifetechnologies, Carlsbad, CA, USA), (d) the remainder of the liver tissue was quickly frozen in liquid nitrogen and stored at −80C.

Liver histology and immunostaining

Tissue sections (5μm) were prepared and routinely stained for hematoxylin and eosin. Steatosis, inflammation and ballooning were scored on the basis of the non-alcoholic fatty liver disease (NAFLD) activity score.[23] Liver fibrosis was assessed with Sirius Red staining. Therefore, liver sections were incubated for 2 h at room temperature with an aqueous

solution of saturated picric acid containing 0.1% Fast Green FCF and 0.1% Direct Red. Terminal deoxynucleotidyl transferase dUTP nick-end labeling (TUNEL) assay was performed per manufacturer's instructions (ApopTag® Peroxidase In Situ Apoptosis Detection Kit, Millipore, Billerica, MA, USA) and quantitated as previously described.[24] Immunohistochemistry straining for myeloperoxidase (Myeloperoxidase Ab-1, Thermo Scientific, Waltham, MA, USA) was performed in formalin-fixed, paraffin-embedded livers according to manufacturer's instruction. Receptor interacting protein kinases 1 and 3 (RIP1 and RIP3) (RIP1, BD610458, BD, Franklin Lakes, NJ, USA; RIP3, sc47364, Santa Cruz Biotechnology, Inc., Santa Cruz, CA, USA) were visualized in 5μm thick liver section via simultaneous double staining immunofluorescence.

Immunoblot analysis

For immunoblot analysis 50mg whole-liver lysate was resolved by a 4–20% gradient gel or 18% gel, transferred to nitrocellulose membrane, and blotted with appropriate primary antibodies. Membranes were incubated with peroxidase-conjugated secondary antibody (dilution 1:10,000) (GeneTex, Irvine, CA, USA), protein bands were visualized with the enhanced chemiluminescence reagent and digitized using a CCD camera (ChemiDoc®, Biorad, Hercules, CA, USA). Expression intensity was quantified by ImageLab (Biorad). Anti-Transforming growth factor-β (TGF-β) antibody (dilution 1:1000) (Cell Signaling), anti-Casp1 p10 (dilution 1:500), anti-IL-18 (dilution 1:500) (both Santa Cruz), and anti-IL-1β (dilution 1:1000) (abcam, Cambridge, MA, USA) were used. Protein load was verified with an α-tubulin antibody (dilution 1:10,000) (Hybridomabank, University of Iowa) (kindly provided by M. Kaulich). IL-1β was quantified in whole liver samples using a mouse IL-1β ELISA (R&D Systems, Minneapolis, MN, USA) according to the manufactures instruction.

Real-time PCR

Total RNA was isolated from liver tissue using an RNeasy Tissue Mini kit (Qiagen, Valencia, CA, USA). The reverse transcript (cDNA) was synthesized from 1μg of total RNA using the iScript cDNA Synthesis kit (Biorad). Real-time PCR quantification was performed using Sybr-Green and CFX96 Thermal Cycler from Biorad. Briefly, 10μl of reaction mix contained: cDNA, KAPA SYBR® FAST qPCR master mix, and primers at final concentrations of 200nmol. The sequences of the primers used for quantitative PCR are given in supplemental table 1.

Flow cytometry

For detailed characterization of the inflammatory infiltrate within the livers of Nlrp3 mutant mice we separated livers and analyzed samples by flow cytometry. Whole livers were force filtered through a 70μm nylon cell strainer (BD) with PBS. The solution was centrifuged for 1min at 8°C with 500rpm producing a pellet of parenchymal cells and a supernatant incorporating the infiltrating cells. The supernatant was applied to Ficoll (Ficoll-Paque™ PLUS, GE Healthcare, Upsalla, Sweden) and centrifuged at 3,000rpm for 25min at room temperature. The layer of mononuclear cells was recovered, incubated with RBC lysis buffer (eBioscience, San Diego, CA, USA), and washed with PBS by centrifugation. Infiltrating cells were classified by multicolour analysis after incubation with CD45 (BD), CD11b

(eBioscience, San Diego, CA, USA), CD11c (eBioscience), CD11b (eBioscience), F4/80 (AbD serotec, Kidlington, UK) and CD4 (eBioscience) for 30min on ice and washed with 3% FBS-PBS. Analysis of RIP1 and RIP3 expression was performed in whole liver lysates of Nlrp3 CreZ mutants utilizing RIP1 (BD) and RIP3 (Santa Cruz) antibodies. Cells were analyzed by flow cytometry (BD LRS II).

Determination of pyroptotic cell death in hepatocytes

To assess pyroptosis *in vivo* we designed the following strategy. Active Caspase 1 was measured in parenchymal cell suspensions with FLICA 660-YVAD-FMK (FLICA® 660 in vitro Active Caspase-1 Detection Kit, ImmunoChemistry Technologie, Bloomington, MN, USA) according to manufactures instructions and with propidium iodide (PI) to mark cells with membrane pores (life technology, Carlsbad, CA, USA). To determine the rate of pyroptotic cell death in hepatocytes we excluded monomorphic cells based on size and positive staining for F4/80 and CD11b from the analysis.

Statistical analyses

Analyses were performed with Graph Pad (version 5.03; Graph Pad Software Inc., La Jolla, CA, USA). Flow cytometry data was analyzed using FlowJo software (version 10.0.5; Tree Star, Inc., Ashland, OR, USA) .The significance level was set at $\alpha = 5\%$ for all comparisons. Wilcoxon rank-sum tests, unpaired t-tests, and Kruskal-Wallis test were used for comparison of continuous variables. Unless otherwise stated, data are expressed as mean +/− SEM or as median and range / quartiles for continuous variables and as absolute number or percentage for categorical variables.

Results

Mutant NLRP3 leads to growth retardation and impaired survival

Nlrp3 CreZ knock-in pups - were born at the expected Mendelian frequency (Fig 1). Although often indistinguishable from wild-type (WT) siblings at birth, Nlrp3 CreZ knock-in mice exhibited growth retardation and significantly lower body weight obvious by post birth day 5.[20] Moreover, Nlrp3 knock-ins developed cutaneous inflammation with concomitant hair loss (Fig 1). Nlrp3 CreZ mice usually died at 2–3 weeks. WT mice showed significantly more weight at time of sacrifice: median weight of WT 9.1g (minimum 7.38g, maximum 11.4 g), Nlrp3 CreZ 3.12g (2.45g, 3.52g) (Fig 1). Notably, Nlrp3 mutants showed significant higher liver weight as a percentage of body weight than aged matches WTs; Nlrp3 CreZ median 6.3%, WT 3.5% (Fig 1).

Active NLPR3 inflammasome results in severe liver inflammation with neutrophil infiltration

Liver histology of Nlrp3 CreZ mutants revealed severe inflammation with many inflammatory foci composed predominantly of polymorphonuclear cells and areas of cell death (Fig 2). Analysis of mRNA showed that Nlrp3 mutants exhibit significantly higher levels of pro-IL1β (Nlrp3 CreZ 6.6-fold change to WT; $p<0.05$), apoptosis-associated speck-like protein containing a caspase recruitment domain (ASC) (3.3-fold; $p<0.05$), Casp1 (3.2-fold; $p<0.05$), and tumor necrosis factor-α (TNF-α) (4.0-fold; $p<0.05$) compared to

WT controls (Fig 2). Whole liver lysates showed a marked increase in IL-1β (8.0-fold; $p<0.05$) and IL-18 (2.0-fold, p = NS) protein expression (Fig 2). To perform a detailed characterization of the inflammatory cell infiltrate in Nlrp3 mutants, we separated residential from infiltrating cells in the liver. Infiltrating cells showed high intensity of CD45 and CD11b staining compared to WT controls; no difference was observed in CD11c, CD4, and CD8 staining; and Nlrp3 CreZ mutants showed less F4/80 intensity (Fig 2). Analysis of whole liver lysates showed no significant difference in F4/80 mRNA levels in Nlrp3 mutants although monocyte chemoattractant protein 1 (MCP-1) was significantly elevated. This result, indicating that neutrophils are the most prevalent infiltrating cell population, was further confirmed by myeloperoxidase (MPO) immunohistochemistry of liver sections (Fig 2). Neutrophil leukocyte recruitment was mediated via a marked increase in chemoattractant (CXCL1, CXCL2 and CXCL5), whereas endothelium expressed leukocyte adhesion molecules (CD47, intercellular adhesion molecule 1 (ICAM1), platelet endothelial cell adhesion molecule 1 (PECAM1)) did not show significant alterations in mutant mice (Fig 2).

To explore whether necroptosis was increased in mutant mice we assessed the expression and activation of kinases receptor-interacting protein (RIP) 1 and RIP3, which have been shown to be required for necroptosis. Livers of Nlrp3 CreZ mice and WT littermates were harvested and stained with RIP1 and RIP3 antibodies and analysed by Flow cytometry. Whole liver lysates of Nlrp3 CreZ mutants showed a slight increase in RIP1 positive cells and no detectable difference in RIP3 positive cells when compared to WT littermates (supplemental Fig. 1). To detect RIP1 - 3 complex formations, required for initiation of nercroptosis, we performed double immunofluorescence staining that demonstrated a lack of co-localization of RIP1 and RIP3 in mutant mice similar to controls (supplemental Fig. 1).

NLRP3 activation results in hepatocyte pyroptosis

Several forms of cell death including oncosis (or necrotic cell death), apoptosis, programmed necrosis (or necroptosis), and autophagic cell death have been recognized to have roles in various acute and chronic liver pathologies. Pyroptosis, a term coined a decade ago by Cookson and Brannan[11], is a novel form of programmed cell death that differs from other types of cell death in that it's dependent on Casp1 activation, results in DNA damage with positivity for TUNEL staining, develops pore formation in the cell membrane resulting in cell swelling and positivity for propidium iodide (PI) staining. Currently pyroptosis, as an additional mechanism to Casp1 dependent processing and activation of pro-inflammatory cytokines, has not been characterized in liver pathologies, nor has its relevance to *in vivo* models been fully elucidated. It has been suggested that pyroptosis may occur in cells (such as hepatocytes) that are not well equipped for secretion of cytokines following inflammasome mediated Casp1 activation.[25]

We initially observed a significant increase in TUNEL positive cells in livers of Nlrp3 mutant mice (Nlrp3 CreZ 2.2-fold change to WT; $p<0.05$) (Fig. 3) suggesting that either apoptosis or pyroptosis was playing a role in liver pathology. We hypothesized that pyroptotic cell death is occurring in hepatocytes with a constitutively activated NRLP3 inflammasome. Pyroptosis was defined by the presence of both active Casp1 and PI

positivity, two key features that define pyroptotic cell death, and measured as aforementioned by flow cytometry. Notably, hepatocyte cell fractions from Nlrp3 CreZ mice showed a marked increase (more than twenty fold) in the number of Casp1 and PI double-positive cells compared to WT animals (Fig 3). Increased Casp1 expression was confirmed by analyzing liver lysates of Nlrp3 mutant mice. Mice with global mutant NLRP3 inflammasome expression showed an 8-fold increase of cleaved Casp1 ($p<0.05$) (Fig. 6).

NLRP3 inflammasome induces hepatic stellate cell (HSC) activation and collagen deposition

The differential findings observed in Nlrp3 mutant mice, which included several aspects of hepatocyte viability and inflammatory signaling, two events that have been linked to HSC activation, led us to further examine the role of the NLRP3 inflammasome in fibrogenesis and fibrosis in the liver. Indeed, Nlrp3 CreZ mutants showed increased collagen deposition, visualized by Sirius red staining in close proximity to inflammatory hot spots (Fig 4). Moreover, Nlrp3 CreZ mutants displayed significantly higher connective tissue growth factor (CTGF) and tissue inhibitor of matrix metalloproteinase 1 (TIMP1) mRNA level compared to WT mice (Fig 4). TGF-β precursor protein, as well as mature TGF-β also showed higher values in Nlrp3 CreZ mice in comparison to WT littermates.

Liver inflammation but not hepatic stellate cell activation is attenuated by IL-1 receptor antagonist treatment in Nlrp3 mutant mice

To assess the role of IL-1R signaling in liver inflammation and activation of hepatic stellate cells we treated Nlrp3 CreZ mutants with an IL-1 receptor antagonist (anakinra) (Fig 5). Treatment with anakinra resulted in an improvement in liver inflammation and a reduction of TUNEL positive cells. Correspondingly, mRNA levels of tumor necrosis factor-α (TNF-α), pro-IL-1β and pro-Casp1 were significantly decreased in anakinra treated mutants when compared to saline injected controls. Notably, markers of hepatic stellate cell activation (CTGF and TIMP1) were not significantly reduced and collagen deposition as assessed by Sirus red staining was unchanged in anakinra treated mice (Fig 5).

Myeloid cell specific mutant mice exhibit a less severe liver phenotype

To characterize the source of the described NLRP3 effects and in particular the role of inflammatory cell derived NLRP3 inflammasome activation in the liver injury observed in global Nlrp3 mutants, we next generated myeloid cell specific Nlrp3 mutants. To achieve this goal we bred intronic *Nlrp3* floxed mice to mice expressing Cre recombinase under control of the lysozyme promoter (CreL), generating mice that only express mutant NLRP3 in cells of myeloid lineage. Phenotypically Nlrp3 CreZ and Nlrp3 CreL mice were similar, although Nlrp3 CreL mice gained more weight and died usually at a slightly older age than global Nlrp3 mutants (Figure 6). Characterization of the liver changes in Nlrp3 CreL mice showed an increase in inflammatory activity, fibrogenesis and fibrosis when compared to WT animals. However, we detected that liver pathology was less severe than that observed in global Nlrp3 mutant mice. Protein levels of mature IL-1β and TGF-β precursors as well as mature TGF-β were raised in comparison to WT mice but were lower than levels in CreZ mice. In order to examine potential mechanisms involved in differences observed between

Nlrp3 CreZ and Nlrp3 CreL mice, we next examined the presence of DNA breakdown by TUNEL assays. We observed significantly less TUNEL positive cells in myeloid specific mutants compared to global mutants (Fig. 6). Moreover, fractionation of livers followed by flow cytometry for quantitation of pyroptosis as aforementioned, demonstrated that hepatocyte pyroptosis occurs at a much lower rate in myeloid specific compared to global mutants (Fig. 6). Correspondingly, levels of cleaved Casp1 p10-fragments were lower in Nlrp3 CreL mutants (3-fold increase to WT, n.s.) compared to Nlrp3 CreZ mutants (8-fold increase, $p<0.05$).

Discussion

The principal findings of this study relate to the role of cell specific NLRP3 inflammasome activation and pyroptotic cell death in liver injury and fibrosis. These results demonstrate that unrestrained NLRP3 activation results in shortened survival, severe liver inflammation, characterized by a predominantly neutrophilic infiltrate and HSC-activation with collagen deposition in the liver. These effects were partially mediated through IL-1R signaling and associated with the presence of hepatocyte pyroptosis. Myeloid cell derived NLRP3 activation resulted in a less severe liver phenotype in the absence of detectable pyroptotic liver cell death. These results identify NLRP3 inflammasome activation and NLRP3 dependent hepatocyte pyroptotic cell death as novel mechanisms of liver injury and fibrosis.

Our current data demonstrates for the first time the presence of pyroptotic cell death in hepatocytes with a constitutively activated NLRP3 inflammasome. Casp1 induced pyroptosis in macrophages has been previously shown to be important in intracellular bacteria clearance *in vivo* independently of IL-1β and IL-18.[26] In addition, Masters et al. discovered pyroptosis in infection-induced cytopenias by studying inflammasome activation in hematopoietic progenitor cells.[27] Using a novel flow cytometry approach we were able to demonstrate that isolated hepatocytes from mice with a globally activated NLRP3 inflammasome showed a marked increase in the number of cells with active Casp1 and cell membrane pores, two central features that define and differentiate pyroptotic cell death from other forms of cell death such as apoptosis and oncosis. Mice with myeloid specific activation of NLRP3 display an absence of pyroptotic hepatocyte cell death and a less severe liver phenotype, while still having increased levels of IL-1β. It is possible that elevated levels of IL-1β could contribute to cell death by other mechanisms such as TNF-α induced cell death as previously reported in hepatocytes.[28] These results strongly suggest an important contribution of pyroptotic hepatocyte cell death to the liver injury and fibrosis observed in Nlrp3 CreZ mutants. Additionally, treatment with an IL-1 receptor antagonist only partially attenuated liver inflammation in CreZ mice, while fibrogenesis was unchanged. Future studies to further characterize the presence and relevance of pyroptotic cell death in liver pathologies using the approach described in this study are warranted.

As shown earlier and confirmed in our study, activation of the NLRL3 inflammasome leads to neutrophilia in the blood and many tissues with high levels of serum inflammatory mediators.[19-20] In the present study we found a marked increase in leukocyte chemoattractants, whereas markers for leukocyte adhesion did not show significant alterations in mutant mice. Neutrophilia could be due in part to reduced pyroptosis, as recent

studies have shown that neutrophils undergo pyroptotic cell death at a much lower rate than other cells.[29] The neutrophilic infiltration also reveals the main feature of the concept of sterile inflammation, which is a major component of a wide range of liver diseases, including ASH, NASH, drug-induced liver injury, and ischemia/reperfusion injury.[30-31] In addition, sterile inflammation leads to the release of toxic mediators that contribute to pathogenesis of these liver diseases.[32-34] IL-1β, the most widely recognized downstream mediator of the NLRP3 inflammasome, has been shown to stimulate collagen expression in a dose dependent manner in fibroblasts.[35] Moreover, transient expression of IL-1β in airway epithelial cells promoted a significant increase in TGF-β and associated deposition of collagen in the lung.[36] Furthermore, HCSs, the myofibroblasts of the liver, can be activated either by IL-1β or IL-18 to induce collagen deposition.[37] HSCs are known as the major source of CTGF in damaged liver and fully activated HSCs are known to release TIMP1, strongly suggesting a key role for HSC-activation in the fibrosis observed in our models.[38, 39] We found enhanced collagen deposition and increased expression of CTGF and TIMP1 in Nlrp3 CreZ mutant mice with early signs of liver fibrosis which was not reversed with anakinra treatment, suggesting a role for mediators other than IL-1β in liver fibrosis. These results are supported by the recent finding that inflammasome components in hepatic stellate cell lines were found to be important in the regulation of various HSCs functions.[40] Furthermore, NLRP3 inflammsome deficiency was associated with protection against carbon tetrachloride or thioacetamide (TAA)-induced liver fibrosis[40] and was found to reduce mortality and liver injury after acetaminophen administration.[41] Future studies to dissect the importance of cell-specific activation of the NLRP3 inflammasome and the role of IL-1 independent NLRP3 pathways contributing to liver inflammation, cell death, and fibrosis are warranted.

In summary, the current studies uncover the role of NLRP3 activation in liver inflammation and fibrosis. The results support a model in which various liver pathologies such as NASH and ASH due to NLRP3 inflammasome activation in hepatocytes and non-parenchymal cells results in induction of pro-inflammatory signaling, hepatocyte pyroptotic cell death and hepatic stellate cell activation, which are then responsible for collagen deposition and fibrosis (Fig. 7). This data provides new insights into the pathogenesis of liver damage, and identifies potential novel molecular targets for therapeutic intervention for these common and potentially serious diseases.

Supplementary Material

Refer to Web version on PubMed Central for supplementary material.

Acknowledgments

The monoclonal alpha-tubulin antibody developed by J. Frankel and E.M. Nelsen was obtained from the Developmental Studies Hybridoma Bank developed under the auspices of the NICHD and maintained by The University of Iowa, Department of Biology, Iowa City, IA 52242. Mutant mice were generated by S. Brydges, J. Mueller, and D. Kastner.

Funding: The work was funded by NIH (DK076852 and DK082451 to AEF and AI52430 to HMH) and German Research Foundation (DFG-grant 173/2-1 to AW)

Abbreviations

ASC	apoptosis-associated speck-like protein containing a caspase recruitment domain
ASH	alcoholic steatohepatitis
Casp1	Caspase 1
CD	cluster of differentiation
CreL/CreZ	Cre recombinase under control of lysozyme / zona pelucida 3
CTGF	connective tissue growth factor
CXCL 1,2,5	chemokine (C-X-C motif) ligand 1,2,5
FACS	fluorescence activated cell sorter
HSC	hepatic stellate cell
ICAM1	intercellular adhesion molecule 1
IL	interleukin
IL-1R	interleukin-1 receptor
MCP-1	monocyte chemoattractant protein 1
MPO	myeloperoxidase
NAFLD	nonalcoholic fatty liver disease
NASH	nonalcoholic steatohepatitis
PECAM1	platelet endothelial cell adhesion molecule 1
PI	propidium iodide
RIP1,3	receptor-interacting protein 1, 3
WT	wild type
TIMP1	tissue inhibitor of matrix metalloproteinase 1
TNF-α	tumor necrosis factor-α
TGF-β	Transforming growth factor-β
TUNEL	Terminal deoxynucleotidyl transferase dUTP nick-end labeling

References

1. Martinon F, Burns K, Tschopp J. The inflammasome: a molecular platform triggering activation of inflammatory caspases and processing of proIL-beta. Molecular cell. 2002; 10:417–426. [PubMed: 12191486]
2. Strowig T, Henao-Mejia J, Elinav E, Flavell R. Inflammasomes in health and disease. Nature. 2012; 481:278–286. [PubMed: 22258606]
3. Szabo G, Csak T. Inflammasomes in liver diseases. Journal of hepatology. 2012; 57:642–654. [PubMed: 22634126]
4. Gross O, Thomas CJ, Guarda G, Tschopp J. The inflammasome: an integrated view. Immunological reviews. 2011; 243:136–151. [PubMed: 21884173]

5. Walker NP, Talanian RV, Brady KD, Dang LC, Bump NJ, Ferenz CR, Franklin S, et al. Crystal structure of the cysteine protease interleukin-1 beta-converting enzyme: a (p20/p10)2 homodimer. Cell. 1994; 78:343–352. [PubMed: 8044845]
6. Yamin TT, Ayala JM, Miller DK. Activation of the native 45-kDa precursor form of interleukin-1-converting enzyme. The Journal of biological chemistry. 1996; 271:13273–13282. [PubMed: 8662843]
7. Wilson KP, Black JA, Thomson JA, Kim EE, Griffith JP, Navia MA, Murcko MA, et al. Structure and mechanism of interleukin-1 beta converting enzyme. Nature. 1994; 370:270–275. [PubMed: 8035875]
8. Shao W, Yeretssian G, Doiron K, Hussain SN, Saleh M. The caspase-1 digestome identifies the glycolysis pathway as a target during infection and septic shock. The Journal of biological chemistry. 2007; 282:36321–36329. [PubMed: 17959595]
9. Keller M, Ruegg A, Werner S, Beer HD. Active caspase-1 is a regulator of unconventional protein secretion. Cell. 2008; 132:818–831. [PubMed: 18329368]
10. Gurcel L, Abrami L, Girardin S, Tschopp J, van der Goot FG. Caspase-1 activation of lipid metabolic pathways in response to bacterial pore-forming toxins promotes cell survival. Cell. 2006; 126:1135–1145. [PubMed: 16990137]
11. Cookson BT, Brennan MA. Pro-inflammatory programmed cell death. Trends in microbiology. 2001; 9:113–114. [PubMed: 11303500]
12. Fink SL, Cookson BT. Apoptosis, pyroptosis, and necrosis: mechanistic description of dead and dying eukaryotic cells. Infection and immunity. 2005; 73:1907–1916. [PubMed: 15784530]
13. Brennan MA, Cookson BT. Salmonella induces macrophage death by caspase-1-dependent necrosis. Molecular microbiology. 2000; 38:31–40. [PubMed: 11029688]
14. Fink SL, Cookson BT. Caspase-1-dependent pore formation during pyroptosis leads to osmotic lysis of infected host macrophages. Cellular microbiology. 2006; 8:1812–1825. [PubMed: 16824040]
15. Dixon LJ, Berk M, Thapaliya S, Papouchado BG, Feldstein AE. Caspase-1-mediated regulation of fibrogenesis in diet-induced steatohepatitis. Laboratory investigation; a journal of technical methods and pathology. 2012; 92:713–723.
16. Petrasek J, Bala S, Csak T, Lippai D, Kodys K, Menashy V, Barrieau M, et al. IL-1 receptor antagonist ameliorates inflammasome-dependent alcoholic steatohepatitis in mice. The Journal of clinical investigation. 2012; 122:3476–3489. [PubMed: 22945633]
17. Csak T, Ganz M, Pespisa J, Kodys K, Dolganiuc A, Szabo G. Fatty acid and endotoxin activate inflammasomes in mouse hepatocytes that release danger signals to stimulate immune cells. Hepatology. 2011; 54:133–144. [PubMed: 21488066]
18. Witek RP, Stone WC, Karaca FG, Syn WK, Pereira TA, Agboola KM, Omenetti A, et al. Pan-caspase inhibitor VX-166 reduces fibrosis in an animal model of nonalcoholic steatohepatitis. Hepatology. 2009; 50:1421–1430. [PubMed: 19676126]
19. Brydges SD, Mueller JL, McGeough MD, Pena CA, Misaghi A, Gandhi C, Putnam CD, et al. Inflammasome-mediated disease animal models reveal roles for innate but not adaptive immunity. Immunity. 2009; 30:875–887. [PubMed: 19501000]
20. Bonar SL, Brydges SD, Mueller JL, McGeough MD, Pena C, Chen D, Grimston SK, et al. Constitutively activated NLRP3 inflammasome causes inflammation and abnormal skeletal development in mice. PloS one. 2012; 7:e35979. [PubMed: 22558291]
21. de Vries WN, Binns LT, Fancher KS, Dean J, Moore R, Kemler R, Knowles BB. Expression of Cre recombinase in mouse oocytes: a means to study maternal effect genes. Genesis. 2000; 26:110–112. [PubMed: 10686600]
22. Clausen BE, Burkhardt C, Reith W, Renkawitz R, Forster I. Conditional gene targeting in macrophages and granulocytes using LysMcre mice. Transgenic research. 1999; 8:265–277. [PubMed: 10621974]
23. Kleiner DE, Brunt EM, Van Natta M, Behling C, Contos MJ, Cummings OW, Ferrell LD, et al. Design and validation of a histological scoring system for nonalcoholic fatty liver disease. Hepatology. 2005; 41:1313–1321. [PubMed: 15915461]

24. Feldstein AE, Canbay A, Guicciardi ME, Higuchi H, Bronk SF, Gores GJ. Diet associated hepatic steatosis sensitizes to Fas mediated liver injury in mice. Journal of hepatology. 2003; 39:978–983. [PubMed: 14642615]
25. Miao EA, Rajan JV, Aderem A. Caspase-1-induced pyroptotic cell death. Immunological reviews. 2011; 243:206–214. [PubMed: 21884178]
26. Miao EA, Leaf IA, Treuting PM, Mao DP, Dors M, Sarkar A, Warren SE, et al. Caspase-1-induced pyroptosis is an innate immune effector mechanism against intracellular bacteria. Nature immunology. 2010; 11:1136–1142. [PubMed: 21057511]
27. Masters SL, Gerlic M, Metcalf D, Preston S, Pellegrini M, O'Donnell JA, McArthur K, et al. NLRP1 inflammasome activation induces pyroptosis of hematopoietic progenitor cells. Immunity. 2012; 37:1009–1023. [PubMed: 23219391]
28. Petrasek J, Dolganiuc A, Csak T, Kurt-Jones EA, Szabo G. Type I interferons protect from Toll-like receptor 9-associated liver injury and regulate IL-1 receptor antagonist in mice. Gastroenterology. 2011; 140:697–708. e694. [PubMed: 20727895]
29. Ceballos-Olvera I, Sahoo M, Miller MA, Del Barrio L, Re F. Inflammasome-dependent pyroptosis and IL-18 protect against Burkholderia pseudomallei lung infection while IL-1beta is deleterious. PLoS pathogens. 2011; 7:e1002452. [PubMed: 22241982]
30. Gao B, Seki E, Brenner DA, Friedman S, Cohen JI, Nagy L, Szabo G, et al. Innate immunity in alcoholic liver disease. American journal of physiology. Gastrointestinal and liver physiology. 2011; 300:G516–525. [PubMed: 21252049]
31. Maher JJ. DAMPs ramp up drug toxicity. The Journal of clinical investigation. 2009; 119:246–249. [PubMed: 19244605]
32. Ohta Y, Imai Y, Matsura T, Kitagawa A, Yamada K. Preventive effect of neutropenia on carbon tetrachloride-induced hepatotoxicity in rats. Journal of applied toxicology : JAT. 2006; 26:178–186. [PubMed: 16278809]
33. Bautista AP. Chronic alcohol intoxication induces hepatic injury through enhanced macrophage inflammatory protein-2 production and intercellular adhesion molecule-1 expression in the liver. Hepatology. 1997; 25:335–342. [PubMed: 9021944]
34. Bonder CS, Ajuebor MN, Zbytnuik LD, Kubes P, Swain MG. Essential role for neutrophil recruitment to the liver in concanavalin A-induced hepatitis. Journal of immunology. 2004; 172:45–53.
35. Postlethwaite AE, Raghow R, Stricklin GP, Poppleton H, Seyer JM, Kang AH. Modulation of fibroblast functions by interleukin 1: increased steady-state accumulation of type I procollagen messenger RNAs and stimulation of other functions but not chemotaxis by human recombinant interleukin 1 alpha and beta. The Journal of cell biology. 1988; 106:311–318. [PubMed: 2828381]
36. Kolb M, Margetts PJ, Anthony DC, Pitossi F, Gauldie J. Transient expression of IL-1beta induces acute lung injury and chronic repair leading to pulmonary fibrosis. The Journal of clinical investigation. 2001; 107:1529–1536. [PubMed: 11413160]
37. Gieling RG, Wallace K, Han YP. Interleukin-1 participates in the progression from liver injury to fibrosis. American journal of physiology. Gastrointestinal and liver physiology. 2009; 296:G1324–1331. [PubMed: 19342509]
38. Liu Y, Meyer C, Muller A, Herweck F, Li Q, Mullenbach R, Mertens PR, et al. IL-13 induces connective tissue growth factor in rat hepatic stellate cells via TGF-beta-independent Smad signaling. Journal of immunology. 2011; 187:2814–2823.
39. Arthur MJ, Mann DA, Iredale JP. Tissue inhibitors of metalloproteinases, hepatic stellate cells and liver fibrosis. Journal of gastroenterology and hepatology. 1998; 13(Suppl):S33–38. [PubMed: 9792032]
40. Watanabe A, Sohail MA, Gomes DA, Hashmi A, Nagata J, Sutterwala FS, Mahmood S, et al. Inflammasome-mediated regulation of hepatic stellate cells. American journal of physiology. Gastrointestinal and liver physiology. 2009; 296:G1248–1257. [PubMed: 19359429]
41. Imaeda AB, Watanabe A, Sohail MA, Mahmood S, Mohamadnejad M, Sutterwala FS, Flavell RA, et al. Acetaminophen-induced hepatotoxicity in mice is dependent on Tlr9 and the Nalp3 inflammasome. The Journal of clinical investigation. 2009; 119:305–314. [PubMed: 19164858]

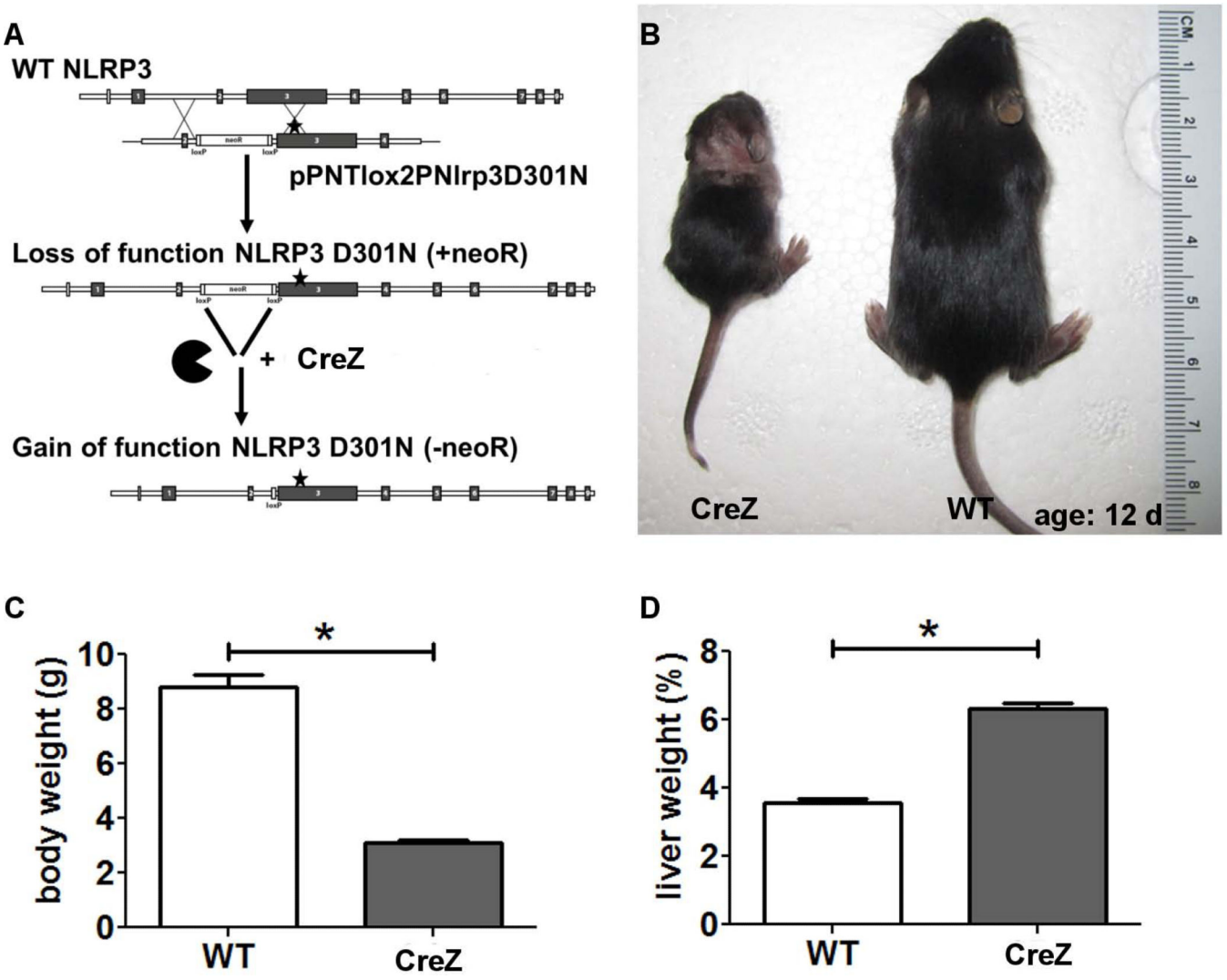

Fig. 1. Nlrp3 knock-ins show growth impairment

Nlrp3 CreZ knock-in pups - with the aspartate 301 to asparagine (D301N) substitution (A) – were often indistinguishable from wild type (WT) siblings at birth but showed growth retardation with significantly lower body weight after 2 weeks (B,C). Notably, Nlrp3 mutants showed significant higher liver weight as a percentage of body weight than WTs; Nlrp3 CreZ median 6.3%, WT 3.5% (D); (n≥7 for each group).

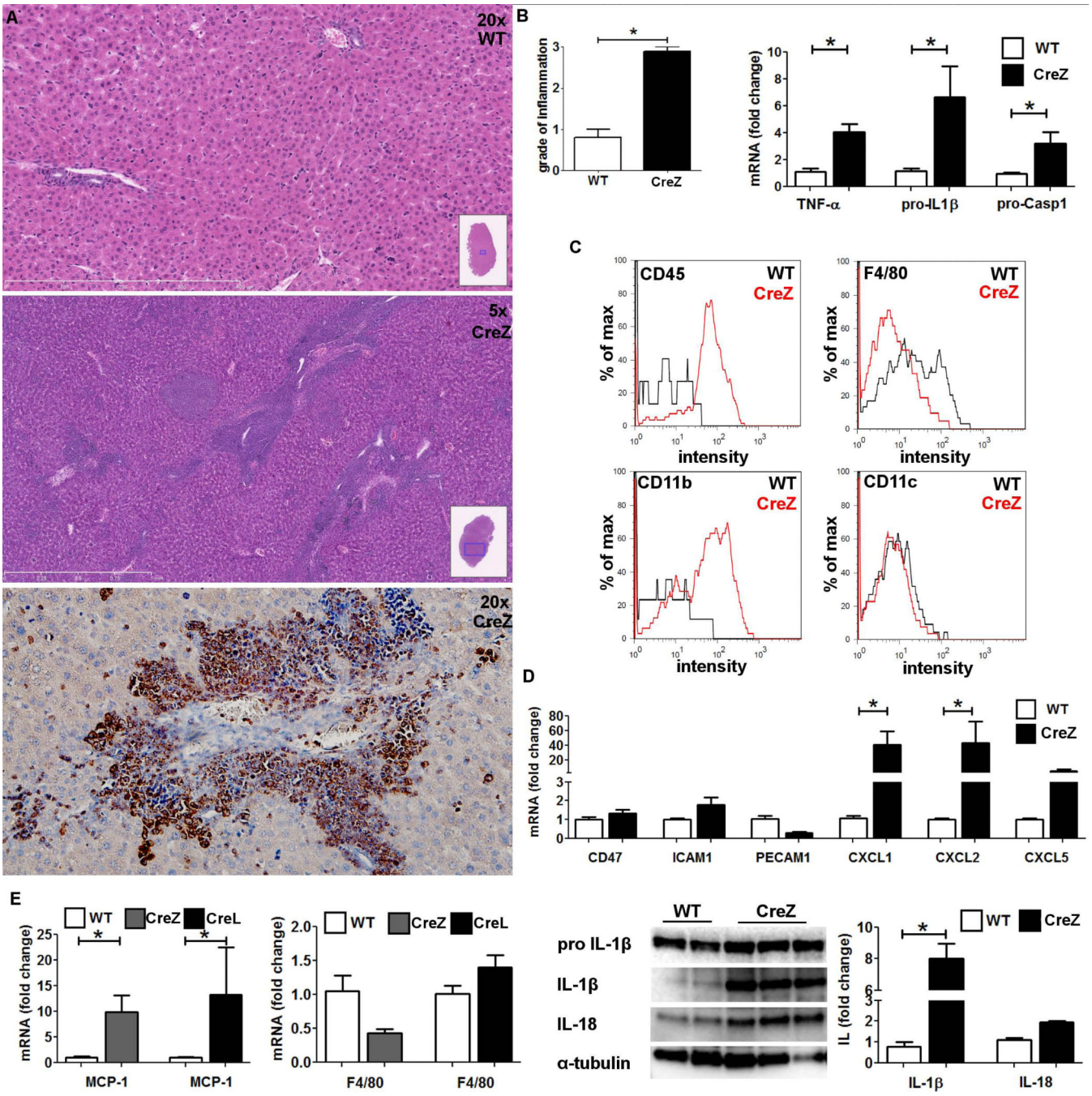

Fig. 2. Global mutant NLPR3 leads to severe liver inflammation

Liver histology of global Nlrp3 knock-ins (CreZ) revealed severe inflammation in comparison to WT littermates, with infiltrating cells being mainly myeloperoxidase positive and therefore classified as neutrophils (representative of 7-13 in each group) (A). Conclusively liver samples of Nlrp3 CreZ mice exhibited significantly higher grade of inflammation scores (B). Moreover, analysis of mRNA levels within whole liver samples showed significantly higher yields of pro-IL1β (Nlrp3 CreZ 6.6-fold change to WT; $p<0.05$), pro-Casp1 (3.2-fold; $p<0.05$), and TNF-α (4.0-fold; $p<0.05$) than WTs ($n\geq7$ for each group) (B). After cell separation infiltrating cells (red curve) of Nlrp3 CreZ mutants showed high intensity in CD45 and CD11b staining compared to WT mice (gray curve); no difference was observed in CD11c, CD4, and CD8 staining; and Nlrp3 CreZ

mutants showed less F4/80 intensity (n≥7 for each group) (C). The neutrophil leukocyte recruitment was mediated via a marked increase in chemoattractants as CXCL1, CXCL2 and CXCL5 whereas endothelium expressed leukocyte adhesion molecules (CD47, ICAM1, PECAM1) did not show significant alterations in Nlrp3 CreZ mice (D) (n≥4 for each group). Analysis of whole liver samples showed no significant differences in F4/80 mRNA levels even though the monocyte chemoattractant protein 1 (MCP-1) was significantly higher in mutant mice with global (CreZ) and myeloid specific (CreL) inflammasome activation (n≥7 for each group) (E). IL-1β and IL-18 protein levels were markedly elevated in whole liver lysates of Nlrp3 CreZ mice (n≥3 for each group) (E).

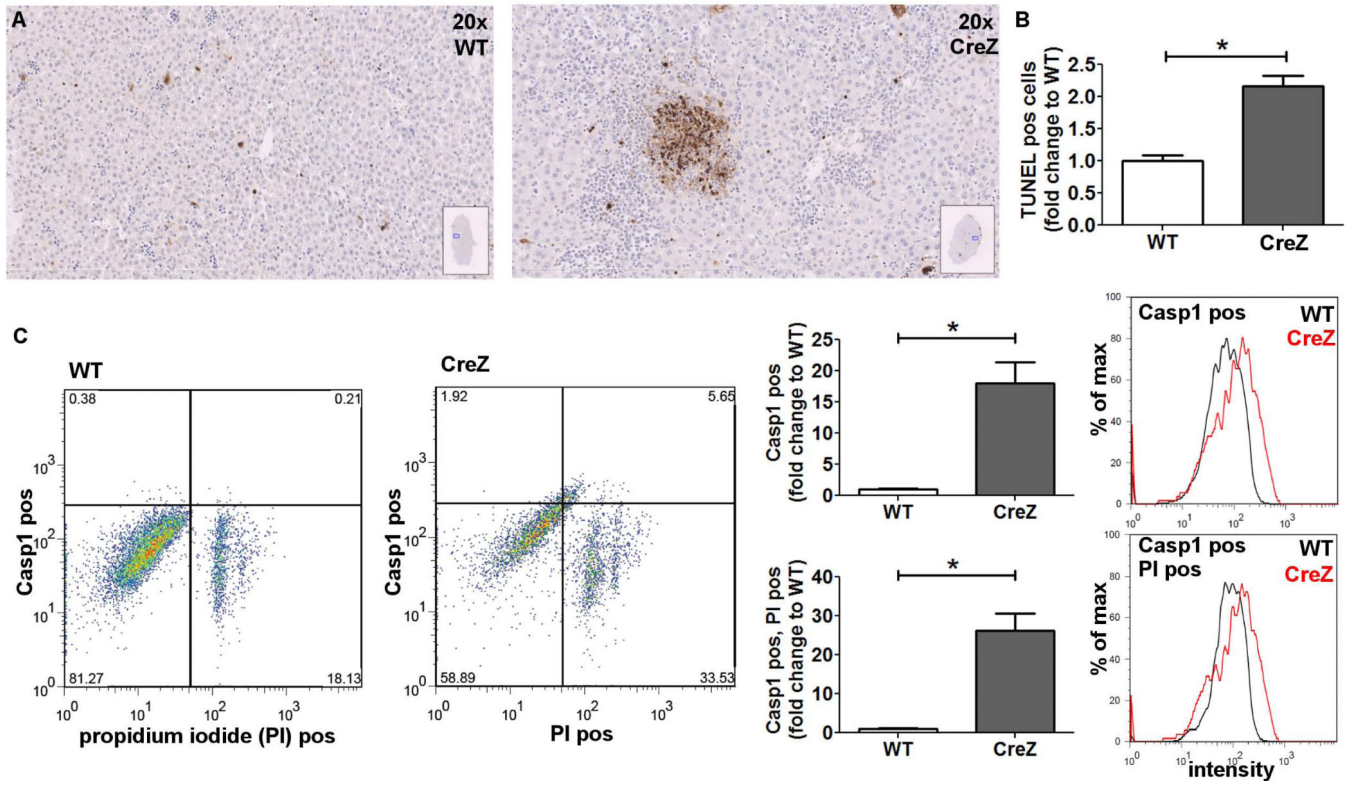

Fig. 3. Global NLRP3 inflammasome activation results in hepatocyte pyroptosis

TUNEL staining of Nlrp3 CreZ mutant liver samples showed significantly more positive cells than WTs. Livers from Nlrp3 CreZ mice displayed TUNEL positive cells throughout the tissue with several dense areas of TUNEL positive cells indicative of pyroptotic cell death (n≥5 for each group) (A, B). Conclusively, Nlrp3 CreZ mutant mice showed more Casp1 and PI double-positive hepatocytes (upper right quadrant) than WT - representative scatterplots are shown in panel C. An approximately fifteenfold increase in Casp1 positive cells was detected in Nlrp3 CreZ (red curve) in comparison to WT (gray curve), the entire population of hepatocytes was analyzed. Casp1 and PI double-positive cells were also detected at a twentyfold increased level in hepatocytes of Nlrp3 CreZ mutants; (n≥7 for each group).

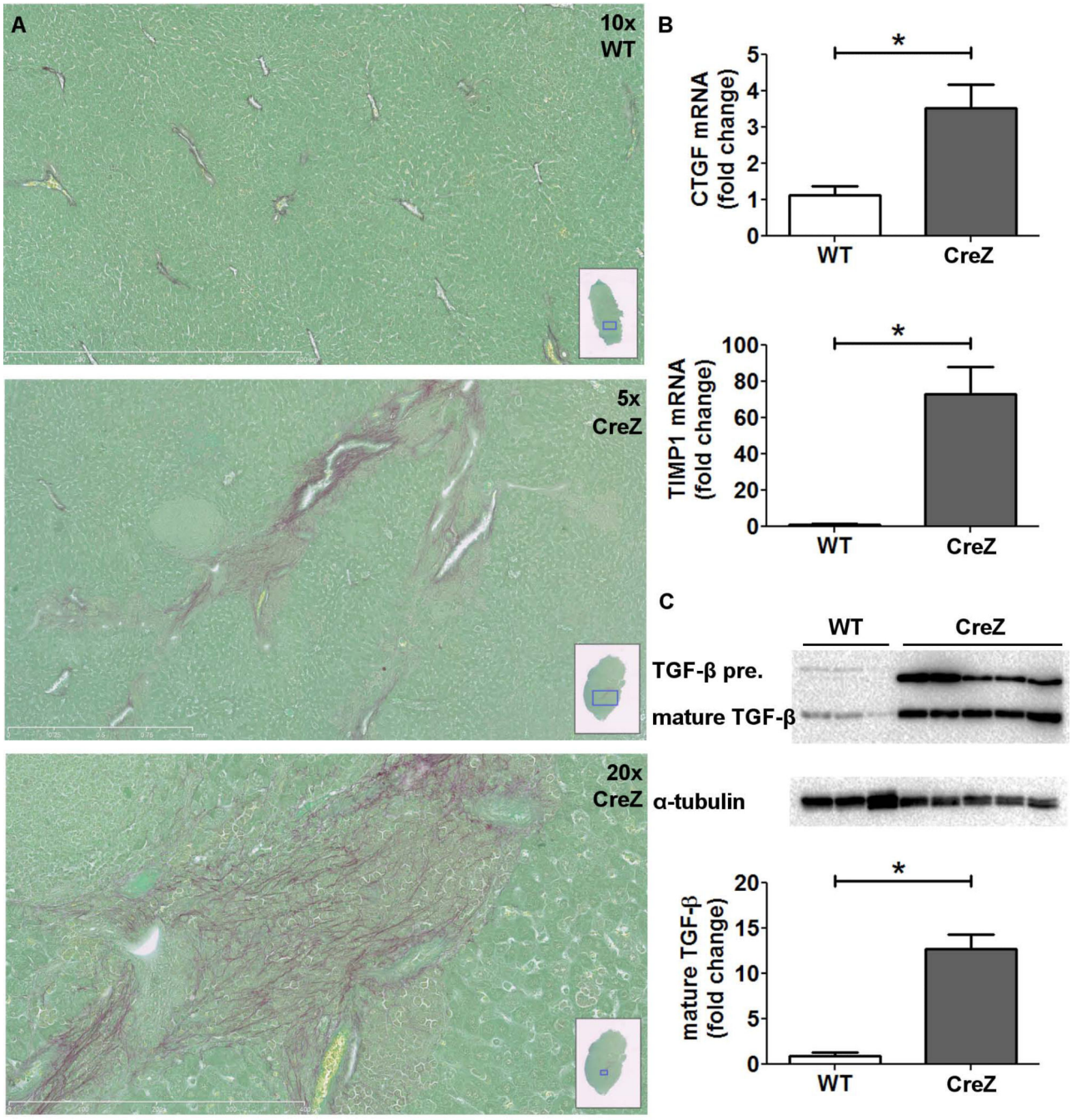

Fig. 4. NLRP3 increases hepatic stellate cell (HSC) activation and spontaneous collagen deposition

Nlrp3 mutants showed increased collagen deposition in comparison to WT littermates visualized by Sirius red staining in close proximity to inflammatory hot spots (A). Moreover, Nlrp3 mutants showed significantly higher CTGF and TIMP1 mRNA levels compared to WT mice (B). TGF-β precursor protein as well as mature TGF-β also showed significantly higher values in Nlrp3 CreZ mice in comparison to WT mice (C); (n≥7 for each group)

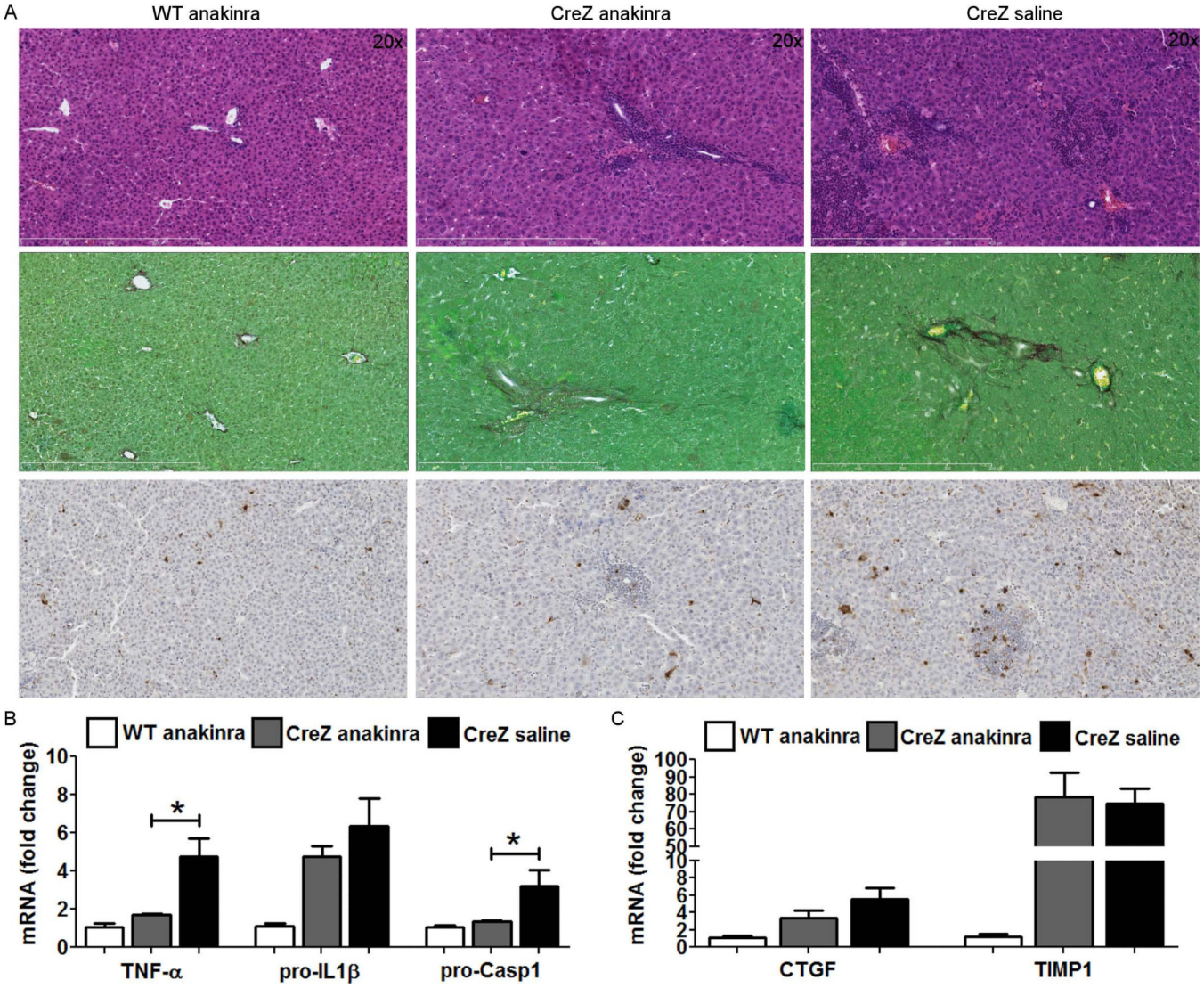

Fig. 5. Treatment with IL-1 receptor antagonist partially attenuates liver pathology in Nlrp3 CreZ mice

Nlrp3 CreZ mutant mice and WT were treated with 300 mg/kg IL-1 receptor antagonist (anakinra) or saline from day 2 to 13. Liver histology of anakinra treated mutants showed a marked decrease in liver inflammation and TUNEL positive cells, whereas collagen deposition assessed by sirius red staining was unaffected (A). Correspondingly, mRNA levels of TNF-α and pro-Casp1 were significantly decreased and mRNA levels of pro-IL-1β showed a trend towards lower levels in anakinra treated mutants in comparison to saline injected mutants (B). Notably, markers of hepatic stellate cell activation, CTGF and TIMP1, were not significantly altered in anakinra treated mice (C); (n≥ 3 for each group).

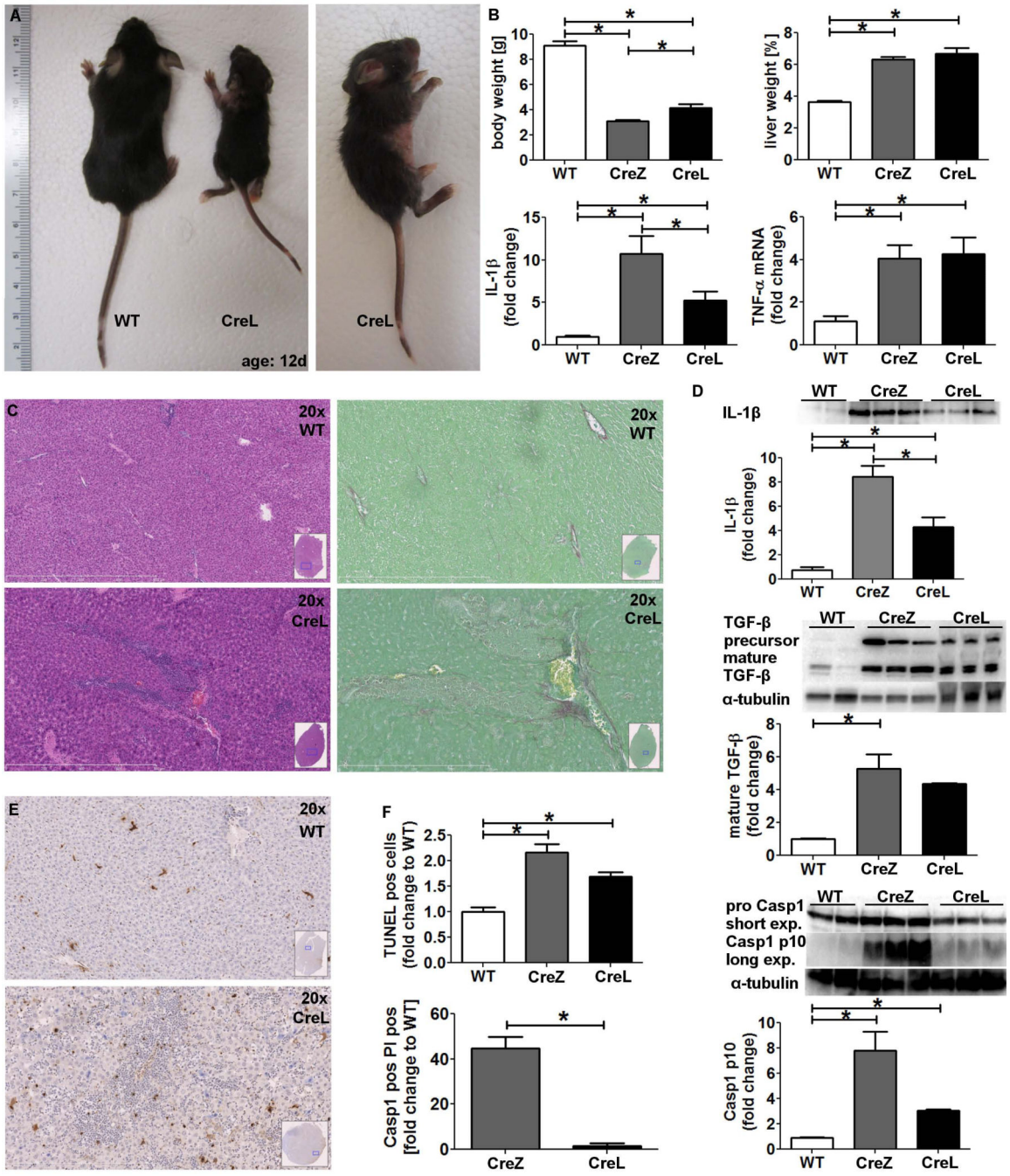

Fig. 6. Myeloid specific mutant NLRP3 generates a less severe liver pathology

Myeloid NLRP3 expression was generated using the lysozyme promoter (CreL) (A). Nlrp3 CreL mice gained slightly more weight (B) and developed marked liver inflammation (C) with less inflammatory hot spots and focal necrosis compared to Nlrp3 CreZ (n≥7 for each group). Level of mature IL-1β of CreL mice was higher than those of WT mice but lower than those of CreZ mice. CTGF and TIMP1 mRNA levels were increased (B) (n≥7 for each group). Nlrp3 CreL mice showed collagen deposition in proximity to inflamed liver areas (C), and an increase in mature TGF-β protein level was documented (D) (n≥3 for each group). Liver samples of myeloid Nlrp3 mutants mice (CreL) showed more TUNEL positive cells than WT controls (E) but less TUNEL positive cells when compared to the global mutants, the latter mainly due to the absence of dense TUNEL positive

regions (F) (n≥7 for each group). Moreover, fractionation of liver into hepatocyte and non-parenchymal fractions followed by flow cytometry for quantitation of pyroptosis as before, demonstrated that hepatocyte pyroptosis occurs at a much lower rate in myeloid specific mutants compared to global mutants (n≥5 for each group) (F). This result was supported by western blot detection of Casp1 p10-fragment which showed significantly higher levels in Nlrp3 CreZ and CreL mice compared to WT littermates (n≥3 for each group).

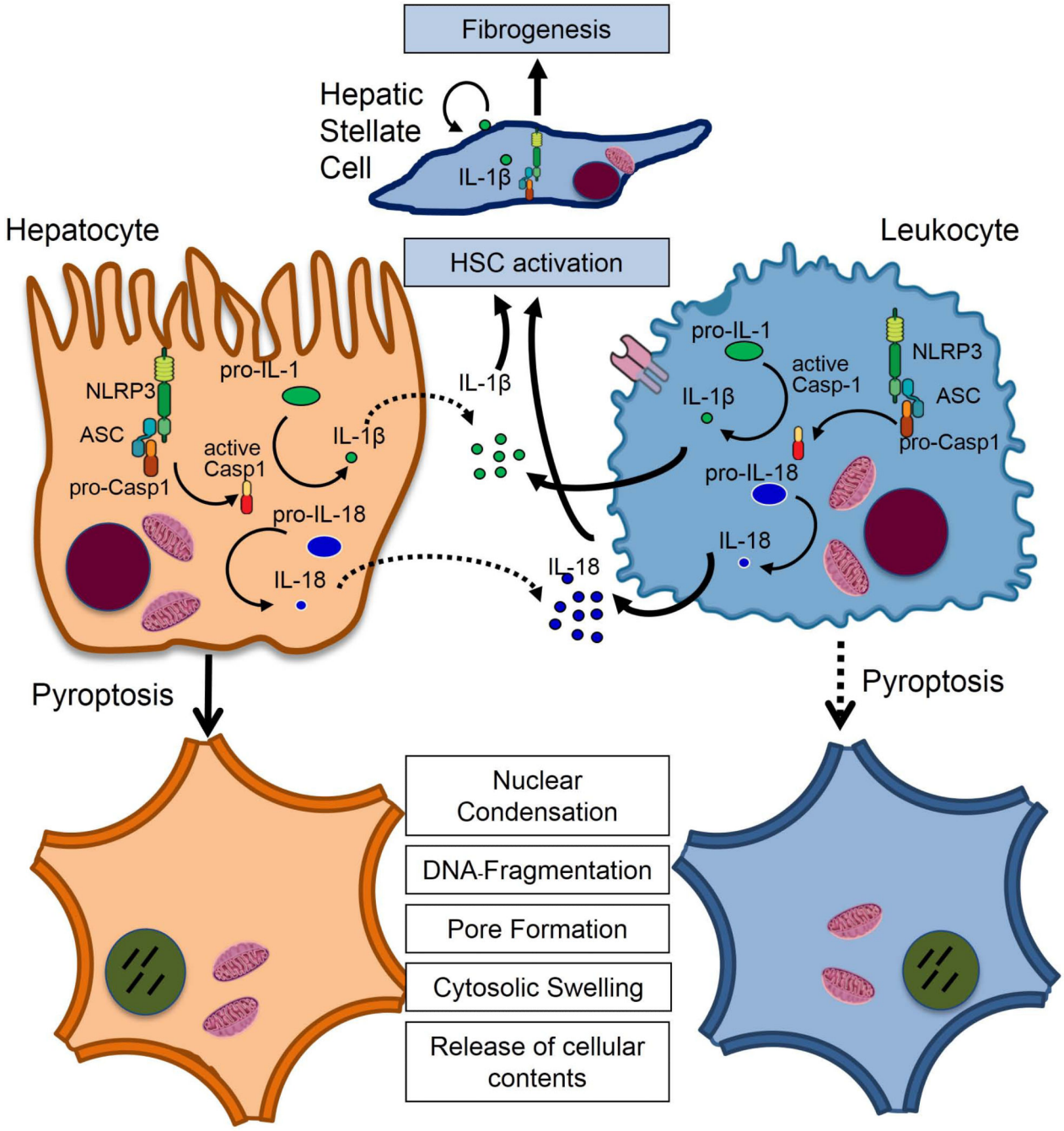

Fig. 7. Model of NLRP3 inflammasome activation in liver disease

Various liver pathologies could induce the NLRP3 inflammasome in hepatocytes and non-parenchymal cells resulting in induction of pro-inflammatory signaling, hepatocyte pyroptotic cell death and hepatic stellate cell activation which are then responsible for collagen deposition and fibrosis. Solid lines represent prominent effects.

Table 1

Effects of NLPR3 inflammasome in global (CreZ) and myeloid cell specific (CreL) mutant mouse models on hepatocytes and hepatic stellate cells. (n.t. not tested).

Model name	Cre recombinase	NLRP3 expression	Liver inflammation	Stellate cell activation	Hepatocyte pyroptosis
Nlrp3 CreZ	Zona Pellucida	global	+++	++	++
Nlrp3 CreL	Lysozyme	myeloid	++	+	<->
Nlrp3 CreZ anakinra treatment	Zona Pellucida	global	+	+	n.t.